Mon. Not. R. Astron. Soc. **321**, 553–558 (2001)

δ Orionis: further temporal variability and evidence for small-scale structure in the interstellar medium

R. J. Price,★ I. A. Crawford and I. D. Howarth
Department of Physics and Astronomy, University College London, Gower Street, London WC1E 6BT

Accepted 2000 September 26. Received 2000 September 25; in original form 2000 August 11

ABSTRACT

We report here the detection of both spatial and temporal variations in interstellar absorption in the line of sight to δ Orionis. First, we present new high-resolution ($R \approx 110\,000$) observations of the interstellar D lines of Na I towards both δ Ori A and C. Comparison of these spectra highlights variations in absorption between the two stars, indicative of small-scale spatial structure in the interstellar medium in this direction over distances of less than $\approx$15 000 au (the projected separation of the two stars). Components with the largest Na I column densities and lowest velocity dispersions are, in general, found to be subject to the greatest differences; in fact the narrowest component detected is only observed in one of the sightlines. This effect has also been reported by Meyer & Blades. Secondly, we present new ultra-high-resolution ($R \approx 900\,000$) Na I D_1 observations and high-resolution ($R \approx 110\,000$) Ca II H & K observations of δ Ori A which, through ultra-high-resolution work conducted between 1994 and 2000, has been shown to exhibit a time-variable interstellar Na I absorption component. These new observations, while revealing the further reduction in intensity of the time-variable Na I absorption, indicate constant Ca II absorption over the same period. This results in a dramatic reduction in the Na°/Ca^{+} abundance ratio, perhaps indicating the line of sight to be gradually probing a less-dense outer region of an absorbing filament.

Key words: line: profiles – stars: individual: δ Ori – ISM: atoms.

1 INTRODUCTION

In recent years it has become clear that the interstellar medium (especially the so-called cold neutral medium) exhibits significant structure on scales of tens to hundreds of astronomical units (reviewed by Heiles 1997). Much of the evidence comes from radio observations of the 21-cm line, through both VLBI observations of extragalactic sources (Dieter, Welch & Romney 1976; Diamond et al. 1989; Davis, Diamond & Goss 1996), and temporal variations of H I absorption towards high-proper-motion pulsars (Frail et al. 1994).

Observations of optical interstellar (IS) absorption lines have also revealed the presence of small-scale structure. Observations of Na I towards the globular cluster M15 made by Meyer & Lauroesch (1999) reveal structure on scale of 2000 to 6000 au. Observations of Na I towards 17 binary/common-proper-motion systems (with projected separations ranging from 480 to 29 000 au) by Watson & Meyer (1996) revealed absorption differences, and therefore structure, in every case. Conversely, observations of Ca II towards binary/common-proper-motion systems showed little evidence of small-scale structure in binaries with separations below 2500 au (Meyer 1990, 1994). The marked difference in the results of the two studies arises from the different conditions which prevail in the regions where such structure is present. Both Meyer & Blades (1996) and Watson & Meyer (1996) find components with the narrower linewidths to display the largest variations; Meyer & Blades also find these components to exhibit larger Na°/Ca^{+} ratios. This suggests the small-scale structure is located in the colder/denser regions, for which Na° is known to be a good tracer, whereas Ca^{+} is expected to be heavily depleted onto grain surfaces (e.g. Barlow & Silk 1977).

Here, observations of δ Orionis, the most westerly of the three stars defining Orion's Belt, and a well-known complex multiple stellar system, are used to probe the small-scale structure in this direction. The O 9.5 II star δ Ori A (HD 36486; $V = 2.2$), which itself is composed of three known components, is accompanied by δ Ori B ($V = 14.0$), which has an angular separation of 33 arcsec, and δ Ori C ($V = 6.85$), at a distance of 52 arcsec. We present new high-resolution observations of the D lines of Na I toward both δ Ori A and C, and observations of the H & K lines of Ca II toward δ Ori A. With a *Hipparcos* distance of 280 pc to these stars (ESA 1997), their angular separation projects to a linear distance of $\approx$15 000 au (0.07 pc). The comparison of Na I absorption arising in these two sightlines reveals marked differences in the

★ E-mail: rjp@star.ucl.ac.uk

line strengths of the components, with one component only detected in one of the sightlines.

In addition, following our earlier detection of a time-variable IS absorption component towards δ Ori A (Price, Crawford & Barlow 2000, hereafter Paper I), we have obtained a new ultra-high-resolution Na I D_1 spectrum of this star. This new observation reveals further changes in the strength of this component.

2 OBSERVATIONS

The observations reported here were obtained at the Mount Stromlo 74-inch telescope (MS74) using the coudé échelle spectrograph with the 130-inch camera (during an observing run in 2000 February 10–22 inclusive), and the Ultra-High-Resolution Facility (UHRF) at the Anglo-Australian Telescope (through service observations on 2000 March 15). Table 1 summarizes the individual observations.

Table 1. Details of each of the exposures made. MS74 and UHRF indicate data obtained with the Mount Stromlo 74-inch telescope and the Ultra-High-Resolution Facility respectively.

Date	Instrument	Target	Region	Exposure (s)
13/02/00	MS74	δ Ori A	Na I D_1/D_2	1000
13/02/00	MS74	δ Ori C	Na I D_1/D_2	1800
15/02/00	MS74	δ Ori C	Na I D_1/D_2	1800
17/02/00	MS74	δ Ori A	Ca II H/K	1800
18/02/00	MS74	δ Ori A	Na I D_1/D_2	1200
19/02/00	MS74	δ Ori C	Na I D_1/D_2	1800
15/03/00	UHRF	δ Ori A	Na I D_1	1800

The MS74 observations were obtained by using a SITe CCD (4096×2048, 15 μm pixels). A slit width of 250 μm was used, providing a velocity resolution (as measured from the width of an unresolved ThAr arc line) of 2.73 km s^{-1} FWHM ($R \approx 110\,000$). The CCD output was binned by a factor of three in the spatial direction in order to reduce the readout noise.

The UHRF observations were obtained by using a Tektronix CCD (1024×1024, 24 μm pixels). The instrument was operated in its highest resolution mode, providing a velocity resolution (as measured from the observed width of a stabilized He–Ne laser line) of 0.34 ± 0.01 km s^{-1} FWHM ($R \approx 880\,000$). The spectrograph was operated with a confocal image slicer (Diego 1993), and the CCD output was binned by a factor of four in the spatial direction in order to reduce the readout noise. Other aspects of the instrument and observing procedures have been described in detail by Diego et al. (1995) and by Barlow et al. (1995).

The spectra were extracted from the individual CCD images using the FIGARO data-reduction package (Shortridge et al. 1999) at the UCL Starlink node. Scattered light and CCD dark current were measured from the inter-order region and subtracted. Wavelength calibration was performed using a Th–Ar lamp, and normalization achieved by division of low-order polynomial fits to the continuum. Removal of telluric water lines from the Na I spectra was achieved by the division by an atmospheric template spectrum. In the case of the MS74 observations, the unreddened star ϵ CMa was observed and its spectrum taken as an atmospheric template. Telluric contamination was removed from the higher resolution UHRF spectra in a similar manner using observations of the lightly reddened star α Vir, as described in more detail in Paper I. Small variations in the strength of the atmospheric lines

Table 2. Velocity systems identified towards δ Ori A & C in the Ca II and Na I regions using MS74 and UHRF data. Signal-to-noise ratios are shown in columns 2 and 8, total equivalent widths are shown in columns 3 and 9. Column 13 contains values of m_s (defined in equation 1). Note that components observed towards δ Ori A & C with the same component number (column 4) in the MS74 Na I data are classified as arising in the same cloud, however the same is not true for comparisons between δ Ori A Ca II, MS74 Na I and UHRF Na I.

Line	S/N	EW (mÅ)	Comp	$v_\odot$ (km s^{-1})	b (km s^{-1}) δ Ori A	log N (cm^{-2})	S/N	EW (mÅ)	$v_\odot$ (km s^{-1})	b (km s^{-1}) δ Ori C	log N (cm^{-2})	m_s
MS74 Data												
Ca II	H: 185	24 ± 1	1	−5.74 ± 0.40	0.50 ± 2.57	9.78 ± 0.25						
	K: 182	44 ± 1	2	4.97 ± 6.00	7.76 ± 4.40	10.94 ± 0.47						
			3	12.29 ± 0.49	4.72 ± 1.46	11.20 ± 0.30						
			4	16.82 ± 0.20	1.64 ± 0.94	10.52 ± 0.35						
			5	21.34 ± 0.07	0.95 ± 0.17	11.07 ± 0.03						
			6	26.00 ± 0.36	4.00 ± 0.83	10.92 ± 0.08						
			7	35.73 ± 1.01	5.05 ± 1.27	10.50 ± 0.10						
Na I	D_1: 192	60 ± 1	1	−0.56 ± 1.46	4.76 ± 1.19	10.68 ± 0.16	60	126 ± 2	−3.77 ± 3.01	4.73 ± 3.01	10.56 ± 0.32	0.14
	D_2: 164	105 ± 1	2	6.50 ± 3.89	3.04 ± 3.25	10.79 ± 0.88	76	206 ± 3	2.00 ± 1.12	2.16 ± 2.31	10.51 ± 0.57	0.31
			3	10.07 ± 1.22	2.25 ± 1.33	10.91 ± 0.63			8.49 ± 0.52	3.28 ± 1.62	11.20 ± 0.17	0.32
			4	–	–	–			11.97 ± 0.09	0.33 ± 0.05	11.55 ± 0.04	1.00
			5	15.59 ± 0.27	2.14 ± 0.52	10.80 ± 0.08			15.48 ± 0.14	1.39 ± 0.34	11.29 ± 0.05	0.51
			6	21.70 ± 0.17	1.34 ± 0.28	11.04 ± 0.06			22.12 ± 1.75	2.08 ± 1.15	11.41 ± 0.48	0.40
			7	25.27 ± 0.09	1.68 ± 0.09	11.50 ± 0.02			24.93 ± 0.34	1.72 ± 0.20	11.96 ± 0.14	0.49
UHRF Data												
Na I	D_1: 82	54 ± 1	1	−4.51 ± 0.39	1.63 ± 0.70	10.20 ± 0.13						
			2	0.58 ± 0.34	2.56 ± 0.92	10.47 ± 0.12						
			3	4.91 ± 0.21	1.29 ± 0.43	10.36 ± 0.17						
			4	9.18 ± 0.16	3.03 ± 0.30	11.01 ± 0.03						
			5	15.03 ± 0.08	1.27 ± 0.14	10.60 ± 0.03						
			6	21.28 ± 0.77	0.49 ± 0.08	10.43 ± 0.15						
			7	22.70 ± 0.05	1.74 ± 0.39	11.04 ± 0.17						
			8	24.88 ± 0.18	1.16 ± 0.25	11.19 ± 0.14						
			9	25.12 ± 0.02	0.31 ± 0.05	10.67 ± 0.09						
			10	26.54 ± 0.02	0.32 ± 0.05	10.56 ± 0.07						

between the different spectra were allowed for by scaling the optical depths of the template atmospheric lines to match those in the δ Ori spectra before division. The spectra were then converted to the heliocentric velocity frame and the individual exposures were added.

An examination of the background levels of the MS74 observations revealed some unexpected variations (by a factor of two or so) between different exposures, and for some exposures of δ Ori C the background contributed up to half of the total counts. Inspection of the raw images revealed that, whatever its cause, this background was constant across the chip in the spatial direction, and that the values measured between the orders are an appropriate correction for the background underlying the orders themselves. Moreover, we have three additional reasons to be confident that the backgrounds in the MS74 data have been dealt with correctly: (1) individual observations of δ Ori C obtained over three nights (Table 1) have different background levels, yet all yield essentially identical line profiles once these backgrounds were subtracted; (2) the MS74 δ Ori A Na I spectrum is identical to the independent UHRF spectrum, after allowing for the difference in resolution; and (3) line-profile analysis (see below) shows that for the δ Ori C Na I spectra, the background removal must be accurate to within $\approx \pm 10$ per cent, as outside this range it proves impossible to model simultaneously the absorption in both D lines. For all these reasons we are confident that the data-reduction process has correctly dealt with the backgrounds, although the relatively high values have adversely affected the signal-to-noise ratio of the δ Ori C observations.

The absorption lines were initially modelled using the IS line-fitting routines in the DIPSO spectral analysis program (Howarth et al. 1993). These models were subsequently optimized through the use of the VAPID routine (Howarth, in preparation) which evaluates a set of component parameters which produce the minimum rms residual. The models have been constructed using a minimum number of absorbing clouds (beyond which the addition of further clouds does not produce a statistically significant improvement to the fit). During the modelling procedure it is possible to fit absorption arising from both the D_1 & D_2, and the H & K transitions simultaneously, in order to produce self-consistent absorption models. The oscillator strengths of the Na I and Ca II transitions were taken from Morton (1991). Hyperfine splitting of the Na doublet has been included in the analysis (see table 4 of Welty, Hobbs & Kulkarni 1994 for details). The resulting line-profile parameters (heliocentric velocity, $v_{\odot}$, velocity dispersion, b, and column density, N) are listed in Table 2.

The best-fitting models for the MS74 spectra, after convolution with the instrumental response function, are shown in Figs 1(a) to (f). Fig. 1(g) shows the UHRF Na I spectrum along with its best-fitting model.

3 DISCUSSION

3.1 Small-scale structure in the direction of δ Orionis

The comparison of the IS Na I spectra of δ Ori A & C (Fig. 1h) reveals substantial differences in the line strengths of the components between the two stars. Such a comparison also reveals the similar velocity structuring of the components, each component observed towards δ Ori A being observed towards δ Ori C with a velocity and velocity dispersion which agree within errors. This highlights the small-scale structure in this direction (at least on these scales) to generally be composed of variations in column density of clouds intersecting both sightlines rather than separate, small clouds present on single sightlines. None of the components are found to be significantly stronger towards δ Ori A. Interestingly, Adams (1949) also found the intensity of Ca II K absorption towards δ Ori C to also be slightly stronger than that towards δ Ori A, consistent with what we observe in Na I.

In order to quantify these differences we have made use of the parameter m_s, introduced by Watson & Meyer (1996) and given by the expression

$$m_s = \left| \frac{N[\mathrm{Na^\circ}]_A - N[\mathrm{Na^\circ}]_C}{N[\mathrm{Na^\circ}]_A + N[\mathrm{Na^\circ}]_C} \right|, \quad (1)$$

where $N[\mathrm{Na^\circ}]_A$ and $N[\mathrm{Na^\circ}]_C$ represent the Na I column densities of paired components towards δ Ori A & C respectively. The final column of Table 2 displays the values of m_s for each component pair. The mean value of m_s is found to be 0.45. This is in the upper range of values found by Watson & Meyer (1996) in their study of 17 sightlines, but agrees with their results when plotted along with the separation of δ Ori A & C in their fig. 2. We note that, in general, those clouds producing absorption components which exhibit the largest differences between sightlines (largest m_s) also have the smallest b-values and largest Na° column densities, an effect also reported by Meyer & Blades (1996) and Watson & Meyer (1996), and attributed to the small-scale structure occurring in colder/denser material.

With a b-value of only $0.33\,\mathrm{km\,s^{-1}}$, component 4 in the MS74 Na I data is the narrowest detected; it is also observed only towards δ Ori C ($m_s = 1$). This strengthens the argument that the observed structure is occurring in cold IS gas since, under the assumption of no turbulence, a strict upper limit of ≈ 150 K can be placed on the kinetic temperature of this cloud. This is in good agreement with the findings of Watson & Meyer (1996), where all but two components with $m_s = 1$ have $b < 1.5\,\mathrm{km\,s^{-1}}$. We note that such a small b-value is well below the instrumental b-value ($1.64\,\mathrm{km\,s^{-1}}$) and so has not been explicitly resolved; however, it is an integral part of the absorption model that statistically provides the best fit to the data. This component is characterized by similar values to that of the time-variable absorption reported towards δ Ori A (attributed to filamentary material in the H I shell around the Orion–Eridanus superbubble; Paper I). Its velocity, although some $10\,\mathrm{km\,s^{-1}}$ lower than the δ Ori A time-variable component, still falls within the range of velocities expected for material contained within the same expanding H I shell and lying on this sightline (cf. the maps presented in fig. 8 of Brown, Hartmann & Burton 1995).

By applying the empirical relationship between N(Na I) and N(H I) of Ferlet, Vidal-Madjar & Gry (1985), and assuming $n_H = 10\,\mathrm{cm^{-3}}$, we find the cloud to have a radial extent of 2.3 pc. Alternatively, by assuming the radial extent of the cloud does not exceed the separation of the stars (0.07 pc), we find $n_H > 3 \times 10^2\,\mathrm{cm^{-3}}$. Similar results are obtained for small-scale structure observed in Na I by Watson & Meyer (1996) who, using the latter assumption, find densities of $n_H \geq 10^3\,\mathrm{cm^{-3}}$ in some cases. However, we note that the relationship between N(Na I) and N(H I) is not well defined at the lower Na° column densities observed here (Welty, Hobbs & Kulkarni 1994). In a study of small-scale structure toward the globular cluster M15, Meyer & Lauroesch (1999) find H I column densities inferred from Na I data to be 10 times higher than estimates from 21-cm observations, suggesting an enhanced Na° column density that does not necessarily trace an increased H I column. Similar findings were made by Bates et al. (1995).

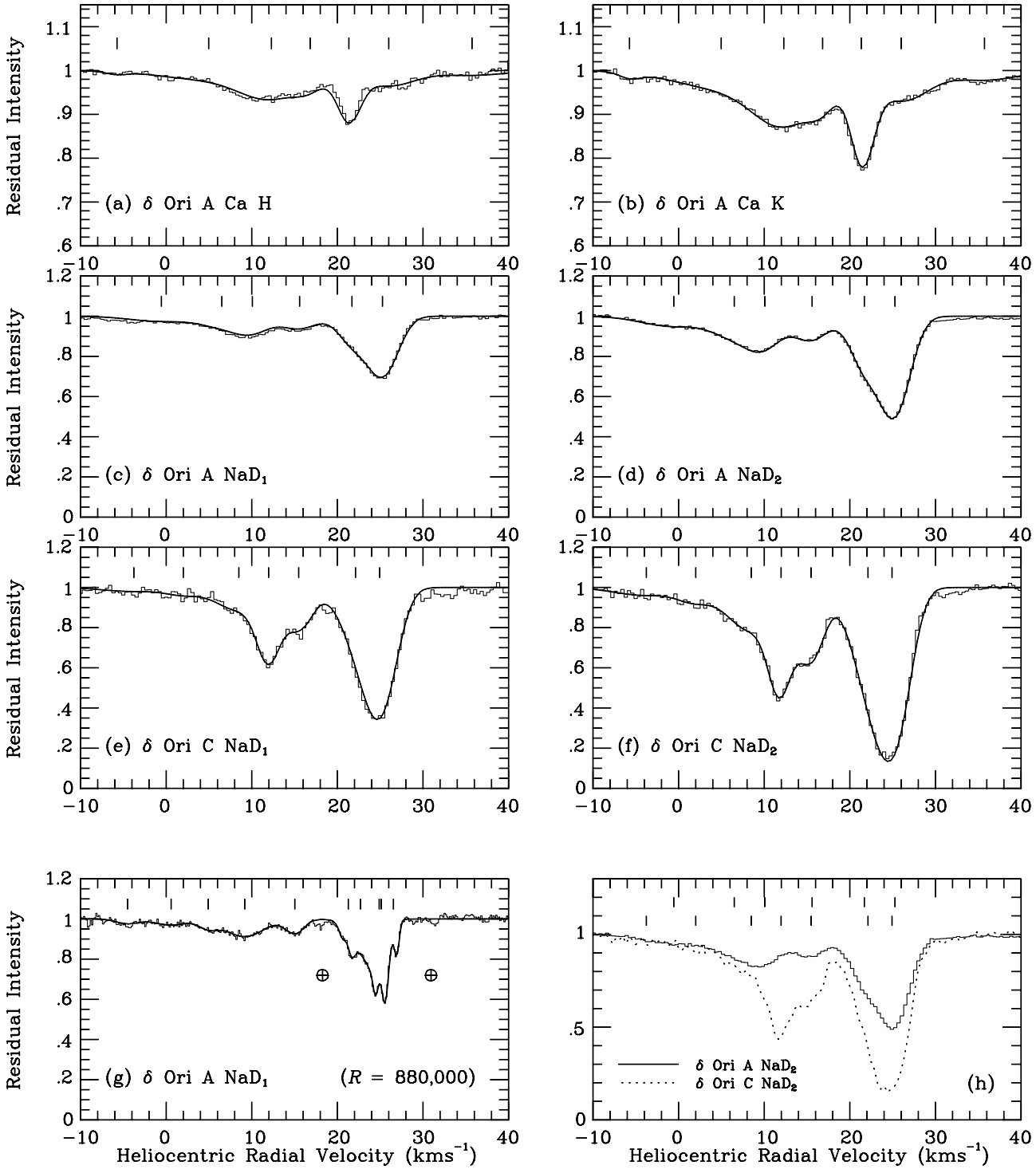

Figure 1. Theoretical line profiles are shown plotted over spectra observed toward δ Ori A in the (a) Ca II H, (b) Ca II K, (c) Na I D_1, (d) Na I D_2, and toward δ Ori C in the (e) Na I D_1, (f) Na I D_2 regions. Frame (g) shows an ultra-high-resolution spectrum of δ Ori A in the Na I D_1 region; the two features indicated with the symbol '$\oplus$' are the locations of residual telluric contamination which has not been fully removed. Frame (h) shows a comparison of the Na I D_2 absorption towards δ Ori A & C, illustrating the presence of small scale structure. The tickmarks indicate the velocities of the individual model components listed in Table 2 (in the case of Frame (h) the upper tickmarks refer to δ Ori A while the lower ones refer to δ Ori C). The poor fit of the model to the 21-km s^{-1} feature in the δ Ori A Ca II H spectrum is a result of an unexplained flat-field feature; however, its excellent fit to the Ca II K absorption (which was modelled simultaneously with the H feature) indicates the model to be accurate. The very weak features present at 32 km s^{-1} in the Na I D_1 & D_2 spectra of δ Ori C have not been modelled but may possibly be authentic, a higher signal-to-noise ratio spectrum is required for their validation.

Table 3. Velocity systems identified towards δ Ori A in the Na I D_1 region using UHRF observations obtained in 1994. Signal-to-noise ratios and total equivalent widths are shown in columns 2 and 3 respectively. Plots of the original 1994 and 1999 Na I spectra can be found in Paper I.

Year/ Line	S/N	EW (mÅ)	Comp	$v_\odot$ (km s^{-1})	b (km s^{-1})	log N (cm^{-2})
1994						
Na I	185	61	1	-4.92 ± 0.12	0.83 ± 0.23	9.86 ± 0.06
			2	0.03 ± 0.34	2.44 ± 0.46	10.37 ± 0.08
			3	4.72 ± 0.20	2.12 ± 0.43	10.52 ± 0.11
			4	9.32 ± 0.12	2.63 ± 0.18	10.96 ± 0.03
			5	15.07 ± 0.04	1.56 ± 0.07	10.68 ± 0.01
			6	21.25 ± 0.53	0.45 ± 0.33	10.94 ± 0.11
			7	22.56 ± 0.01	2.41 ± 0.01	11.12 ± 0.02
			8	24.85 ± 0.07	1.38 ± 0.15	11.16 ± 0.10
			9	25.11 ± 0.01	0.36 ± 0.02	10.74 ± 0.04
			10	26.57 ± 0.01	0.38 ± 0.03	10.54 ± 0.04
1999						
Na I	31	60 ± 3	6	21.26 ± 0.07	0.44 ± 0.09	10.60 ± 0.05
2000						
Na I	82	54 ± 1	6	21.39 ± 0.05	0.39 ± 0.06	10.24 ± 0.04

Furthermore, although observations of Na I towards the binary μ Cru by Meyer & Blades (1996) identified significant structure, subsequent observations of Na I, C I, Mg I, Cr II and Zn II made by Lauroesch et al. (1998) were able to show two things: (1) only the neutral species exhibit these *spatial* variations strongly, and (2) Na I experienced no *temporal* variability in the 21 months between observations. Point (1) is best interpreted as being due to a change of ionization state, rather than total column density, and indicates that the line of sight to μ^1 Cru passes through a denser, colder core (with a higher recombination rate) within a larger cloud which is seen towards both μ^1 and μ^2 Cru.

Indeed, in his extensive study of small-scale structure in the interstellar medium (ISM), Heiles (1997) has argued persuasively that the material responsible must exist in the form of non-spherical clouds, which are postulated to be in the form of cold ($T \approx 15$ K) and dense ($n_H \approx 10^3$ cm^{-3}) curved sheets or filaments. These structures are distributed through the cold neutral medium with random orientations, separated by warmer, less-dense material. When such sheets/filaments are aligned along the line of sight it becomes possible to achieve large variations in column density over small transverse scales without requiring implausibly high spatial densities. Additionally, the conditions prevailing in such structures would lead to an enhanced recombination rate causing the less highly ionized species (such as Na°) to become further enhanced. The differences in the strengths of the various Na I absorption components towards δ Ori A and C may well result from a similar cause.

In principle, the Na°/Ca$^+$ ratio can also be used to estimate the density and ionization conditions in IS clouds (e.g. Crawford 1992, and references therein). However, we are, unfortunately, lacking observations of Ca II towards δ Ori C, so this analysis cannot yet be performed in this case. The particular case of the Na°/Ca$^+$ ratio of the *variable* absorption component towards δ Ori A is discussed below.

3.2 δ Ori A transient absorption

Following the detection of a time-variable absorption component toward δ Ori A (reported in Paper I), a further UHRF spectrum of the Na I D_1 region has been obtained, and illustrates a significant change in column density for this component over a period of less than 1 yr. The new spectrum has been modelled, producing the parameters listed in Table 2, and the model fit shown in Fig. 1(g). An absorption model has also been produced with all parameters, apart from those of the transient component, fixed to those found by modelling the higher S/N 1994 Na I D_1 spectrum, which, apart from the transient component, looks identical. Table 3 lists the parameters for the optimized model fit to the 1994 data (these model parameters differ from those published previously since the VAPID routine shows that the blended absorption between ≈20 & 30 km s^{-1} can be fitted with five rather than six components), along with the parameters for the transient component in 1999 and 2000. Fig. 2 illustrates the variations graphically.

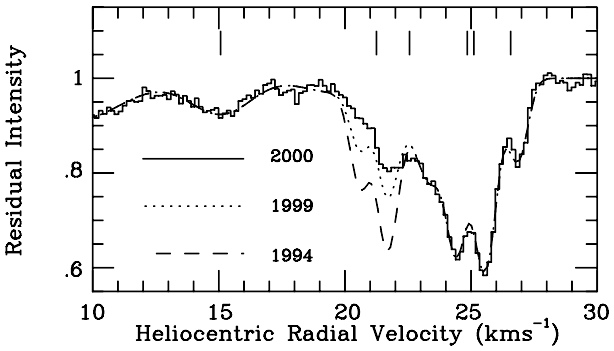

Figure 2. A comparison of the UHRF Na I D_1 spectrum observed toward δ Ori A in 2000 (solid line) with the absorption models for UHRF spectra obtained in 1999 (dotted line) and 1994 (dashed line). Plots of the original 1994 and 1999 Na I spectra can be found in Paper I. The tickmarks indicate the velocities of the individual model components listed in Table 3.

A comparison of the MS74 Ca II data with two previously published Ca II spectra (Paper I and Welty, Morton & Hobbs 1996; both of which were obtained in 1994) shows that there has been no significant change in the line profile. This is for a period where the column density of Na° was seen to decrease by a factor of 4.5. This has, of course, resulted in a decrease in the Na°/Ca$^+$ ratio by the same factor, from 0.63 ± 0.18 in 1994 to 0.15 ± 0.02 in 2000. The first thing to note is that even the higher of these values is still a fairly low ratio by cold neutral medium standards, where values >1 (sometimes $\gg 1$) are generally found owing to the preferential depletion of Ca on to grain surfaces (e.g. Crawford 1992, and

references therein). As discussed in Paper I, this relatively low ratio suggests an origin in either a low-density medium ($n \sim 10\,\mathrm{cm}^{-3}$), or a denser environment within which adsorbed Ca atoms have been partially removed from the grain surfaces. The latter possibility strengthens the suggestion made in Paper I that this component possibly arises in shocked material associated with the Orion–Eridanus shell.

However, the fact that the observed change in $\mathrm{Na}^{\circ}/\mathrm{Ca}^{+}$ is solely as a result of a reduction in Na°, rather than an increase in Ca^{+}, means that it cannot be interpreted simply as the line-of-sight sampling a region of less extreme Ca depletion. Following Heiles (1997), it seems more likely that we are here observing the gradual reduction of the Na^{+} to Na^{0} recombination rate as the line of sight gradually moves away from a high-density filament within which the recombination rate was enhanced. While at first sight such a situation might be expected also to result in a decrease in Ca II (owing to reduced recombination of Ca^{++} to Ca^{+}), in practice Ca is probably sufficiently depleted that this effect is masked by Ca II arising in warmer, more diffuse regions of the cloud (e.g. Crinklaw, Federman & Joseph 1994). It must be noted, however, that over the earlier period 1970 to 1994, when the Na° column density in this component increased substantially, there *is* evidence for a corresponding increase in the strength of Ca II (see fig 2 of Paper I). Thus the Ca^{+} column density cannot be completely insensitive to changing physical conditions over small spatial scales.

4 CONCLUSIONS

We have presented observations which clearly demonstrate variations in the strengths of interstellar absorption lines between two stars in the well known multiple system δ Orionis. The two stars, δ Ori A & C, are separated by 52 arcsec which corresponds to a projected separation of 15000 au (0.07 pc). The magnitude of the column-density differences vary between components, and it is notable that the narrower/stronger components are observed to exhibit the greatest differences. Indeed, the narrowest component detected is only present towards one of the stars.

Although these line-of-sight variations, detected in Na I, may trace differences in the spatial extent and/or density of the absorbing clouds, they may also reflect changes in the ionization equilibria owing to changes in the prevailing physical conditions (e.g. temperature, electron density and local radiation field). In any case, these observations add weight to the view that small-scale density variations are ubiquitous in the ISM (e.g. Heiles 1997, and references therein).

We have also presented observations demonstrating further changes in a previously reported variable interstellar component towards δ Ori A (Paper I) – further reduction in the intensity of the component at $21.3\,\mathrm{km\,s}^{-1}$ has occurred over only one year. This change is interpreted as being due to a reduced recombination rate as the line of sight probes closer to the edge of a dense filamentary structure of the kind postulated by Heiles (1997).

It is notable that while significant differences exist in the strength of the interstellar absorption components identified towards δ Ori A and C, only one (that at $+21.3\,\mathrm{km\,s}^{-1}$) exhibits temporal variability over the period considered here. As discussed in Paper I, this component has a radial velocity consistent with it arising in a swept-up shell at the periphery of the Orion–Eridanus superbubble, where high tangential velocities might be expected. This would also be consistent with the low $\mathrm{Na}^{\circ}/\mathrm{Ca}^{+}$ ratio of this component. Thus, while most of the (apparently non-variable) differences between these two neighbouring sightlines can be attributed to the seemingly ubiquitous small-scale structure in the cold neutral medium (Heiles 1997), it seems likely that the *variable* component towards δ Ori A has an origin specifically related to the Orion–Eridanus shell.

ACKNOWLEDGMENTS

We thank the Mount Stromlo Observatory for the award of telescope time, and the staff of the Observatory for their help in setting up the spectrograph. We thank Dr Raylee Stathakis of the AAO for obtaining the UHRF service observation of δ Ori A. RJP and IAC thank PPARC for the award of a Research Studentship and Advanced Fellowship, respectively.

REFERENCES

Adams W. S., 1949, ApJ, 109, 354
Barlow M. J.,Silk J.,ApJ, 211, 83
Barlow M. J., Crawford I. A., Diego F., Dryburgh M., Fish A. C., Howarth I. D., Spyromilio J., Walker D. D., 1995, MNRAS, 272, 333
Bates B., Shaw C. R., Kemp S. N., Keenan F. P., Davies R. D., 1995, ApJ, 444, 672
Brown A. G. A., Hartmann D., Burton W. B., 1995, A&A, 300, 903
Crawford I. A., 1992, MNRAS, 259, 47
Crinklaw G., Federman S. R., Joseph C. L., 1994, ApJ, 424, 748
Davis R. J., Diamond P. J., Goss W. M., 1996, MNRAS, 283, 1105
Diamond P. J., Goss W. M., Romney J. D., Booth R. S., Kalberla P. M. W., Mebold U., 1989, ApJ, 347, 302
Diego F., 1993, Appl. Opt., 32, 6284
Diego F., et al., 1995, MNRAS, 272, 323
Dieter N. H., Welch W. J., Romney J. D., 1976, ApJ, 206, L113
ESA, 1997, The *Hipparcos* and *Tycho* Catalogues, ESA SP-1200
Ferlet R., Vidal-Madjar A., Gry C., 1985, ApJ, 298, 838
Frail D. A., Weisberg J. M., Cordes J. M., Mathers C., 1994, ApJ, 436, 144
Heiles C., 1997, ApJ, 481, 193
Howarth I. D., Murray J., Mills D., 1993, Starlink User Note No. 50,
Lauroesch J. T., Meyer D. M., Watson J. K., Blades J. C., 1998, ApJ, 507, L89
Meyer D. M., 1990, ApJ, 364, L5
Meyer D. M., 1994, in Cutri R. M., Latter W. B., eds, The First Symposium on the Infrared Cirrus and Diffuse Interstellar Clouds, ASP Conf. Ser., 58. Astron. Soc. Pac., San Francisco, p. 3
Meyer D. M., Blades J. C., 1996, ApJ, 464, L179
Meyer D. M., Lauroesch J. T., 1999, ApJ, 520, L103
Morton D. C., 1991, ApJS, 77, 119
Price R. J., Crawford I. A., Barlow M. J., 2000, MNRAS, 312, L43 (Paper I)
Shortridge K. et al., 1999, Starlink User Note No. 86.17
Watson J. K., Meyer D. M., 1996, ApJ, 473, L127
Welty D. E., Hobbs L. M., Kulkarni V. P., 1994, ApJ, 436, 152
Welty D. E., Morton D. C., Hobbs L. M., 1996, ApJS, 106, 533

This paper has been typeset from a TEX/LATEX file prepared by the author.